

Properties of polyamorphous Ce₇₅Al₂₅ metallic glasses

Q. S. Zeng (曾桥石),^{1,2,3,*} V. V. Struzhkin,⁴ Y. Z. Fang,^{5,6} C. X. Gao,⁷ H. B. Luo,^{1,2} X. D. Wang,^{1,2} C. Lathe,⁸ Wendy L. Mao,^{1,2,9,10,11} F. M. Wu,⁵ H.-K. Mao,^{1,2,3,4} and J. Z. Jiang^{1,2,†}

¹International Center for New-Structured Materials (ICNSM), Zhejiang University, Hangzhou 310027, China

²Laboratory of New-Structured Materials, Department of Materials Science and Engineering, Zhejiang University, Hangzhou 310027, China

³HPSynC, Geophysical Laboratory, Carnegie Institution of Washington, Argonne, Illinois 60439, USA

⁴Geophysical Laboratory, Carnegie Institution of Washington, Washington, DC 20015, USA

⁵College of Mathematics, Physics and Information Engineering, Zhejiang Normal University, Jinhua 321004, China

⁶School of Material Science and Engineering, Xi'an University of Architecture and Technology, Xi'an 710055, China

⁷State Key Lab for Superhard Materials, Jilin University, Changchun 130012, China

⁸HASYLAB am DESY, Notkestrasse 85, D-22603 Hamburg, Germany

⁹Geological & Environmental Sciences, Stanford University, Stanford, California 94305, USA

¹⁰Photon Science SLAC National Accelerator Laboratory, Menlo Park, California 94025, USA

¹¹Stanford Institute for Materials and Energy Science, SLAC National Accelerator Laboratory, Menlo Park, California 94025, USA

(Received 1 May 2010; revised manuscript received 28 June 2010; published 17 August 2010)

The thermal stability and electronic transport properties of polyamorphous Ce₇₅Al₂₅ metallic glass (MG) have been investigated using *in situ* high-pressure, high-temperature, energy-dispersive synchrotron x-ray diffraction and *in situ* high-pressure and low-temperature, four-probe resistance measurements. The results are compared with the properties of La₇₅Al₂₅ MG. The pressure dependence of the crystallization temperature and resistance of the Ce₇₅Al₂₅ MG exhibited turning points at the polyamorphic transition pressure, 1.5 GPa, and they clearly presented different behaviors below and above 1.5 GPa. In contrast, no turning points were observed in the La₇₅Al₂₅ MG (La has no 4*f* electron). Additionally, the pressure-tuned temperature coefficient of resistance of the Ce₇₅Al₂₅ MG was observed. These results revealed switchable properties in the polyamorphous Ce₇₅Al₂₅ MG that are linked with 4*f* electron delocalization.

DOI: [10.1103/PhysRevB.82.054111](https://doi.org/10.1103/PhysRevB.82.054111)

PACS number(s): 81.30.Hd, 65.60.+a, 72.15.Cz, 81.05.Kf

Metallic glasses (MGs) with disordered structures exhibit many unique properties that put these materials at the forefront of materials research.^{1,2} Phase transitions in materials often cause a change in their properties, e.g., mechanical, thermal, electrical, magnetic, or optical properties, which could be employed to produce switchable engineered materials, e.g., shape memory alloys, phase-change rewriteable storage, thermal magnetic switchers, etc. Polyamorphism,^{3,4} in which multiple distinct amorphous phases (states) are formed from the same substance, has been extensively investigated in nonmetallic amorphous systems, e.g., amorphous ice,^{5,6} oxides,^{7–11} chalcogenides,^{12,13} silicon,¹⁴ etc. These amorphous materials generally have directional and low-coordination (<6) local environments. The polyamorphic transition from a low-density amorphous (LDA) state to a high-density amorphous (HDA) state under pressure often results from increased atomic coordination and was thought to be impossible in MGs, which most likely have densely packed atomic structures with the maximum coordination number (11–14) among random nearest neighbors.¹⁵

Surprisingly, pressure-induced polyamorphic transitions were recently discovered in Ce-bearing MGs.^{16–18} These results raise an interesting question: which of the unique properties of MGs can be tuned by the polyamorphic transition and how? Until now, only Liu *et al.*¹⁹ have reported electrical resistance and thermometric measurements on La₆₈Al₁₀Cu₂₀Co₂ and Nd₆₀Al₁₀Ni₁₀Cu₂₀ bulk MGs (BMGs) under high pressure, and the two materials presented sharp changes in resistance at about 1.4 GPa and 1.1 GPa, respec-

tively. These changes in resistance were claimed to be due to polyamorphic transitions in La₆₈Al₁₀Cu₂₀Co₂ and Nd₆₀Al₁₀Ni₁₀Cu₂₀ BMGs, although no direct experimental evidence for pressure-induced polyamorphic transitions in either BMG was reported. According to results obtained from *ab initio* calculations and experiments,^{16–18,20,21} the unique polyamorphic transition in Ce-bearing MGs is due to 4*f* electron delocalization under pressure. Thus, it is puzzling to observe similar polyamorphism in the La₆₈Al₁₀Cu₂₀Co₂ MG, which has no 4*f* electrons. Furthermore, x-ray diffraction (XRD) results, taken at pressures up to 40 GPa, suggested no transition for La₇₅Al₂₅ MG under high pressure.²² Very recently, Zeng *et al.*¹⁸ experimentally confirmed an electronic polyamorphic transition at 1.5 GPa in the Ce₇₅Al₂₅ MG. Thus, it is very desirable to examine the differences in the properties of the LDA and HDA MGs. In this work, we investigated the crystallization behavior and resistance of the Ce₇₅Al₂₅ MG, as a prototype system, along with the La₇₅Al₂₅ MG for comparison, using *in situ* high-pressure, high-temperature energy-dispersive x-ray diffraction (HPHT-EDXRD) and *in situ* high-pressure, low-temperature four-probe resistance measurements to address whether properties change at the polyamorphic transition in the polyamorphous Ce₇₅Al₂₅ MG. Different thermodynamic and electrical transport properties are clearly revealed in the LDA and HDA Ce₇₅Al₂₅ MG, linked to 4*f* electron delocalization in Ce-bearing MGs. These findings might promote potential applications that utilize the LDA and HDA MGs.

Ce₇₅Al₂₅ and La₇₅Al₂₅ MG ribbons with a thickness of

about 25 μm and a width of about 1.5 mm were prepared through single-roller melt spinning. Master ingots were prepared by arc-melting a mixture of pure cerium (99.5at. %), lanthanum (99.5at. %), and aluminum (99.95at. %) in a zirconium-gettered argon atmosphere. They were remelted five times to ensure homogeneity in the composition. The pressure dependences of the crystallization onset temperatures (T_x) of the $\text{Ce}_{75}\text{Al}_{25}$ and $\text{La}_{75}\text{Al}_{25}$ MG were measured from about 0.1 to 4.2 GPa by *in situ* HPHT-EDXRD. The measurements were performed with a multianvil pressure apparatus in a 250-ton hydraulic press and synchrotron radiation x rays from the MAX80 beamline at HASYLAB in Hamburg, Germany.²³ Hexagonal boron nitride (BN) powder was used as the pressure medium. The diffraction angle θ was set at 4.514° . The temperature was measured by a thermocouple with a stability of ± 1 K. Each run consisted of an isothermal room-temperature compression stage followed by isobaric heating to high temperature at a rate of 15 K/min. The pressure of the sample was calculated from the lattice constant of NaCl using the Decker equation of state.²⁴ The HPHT-EDXRD patterns were recorded every 20 s to monitor the crystallization at different pressures. The uncertainty in the estimated T_x under pressure was about 5 K. The T_x values of the $\text{Ce}_{75}\text{Al}_{25}$ and $\text{La}_{75}\text{Al}_{25}$ MGs were measured at ambient pressure by a differential scanning calorimeter (DSC) (Perkin-Elmer DSC-7) with a heating rate of 20 K/min in Ar flow. The *in situ* high-pressure, low-temperature four-probe resistance measurements were performed with both a manual four-probe-electrode circuit^{25,26} and an integrated microcircuit²⁷ in a Mao-type diamond anvil cell (DAC) and a L-He cryostat. In the manual four-probe-electrode circuit method, the T301 gasket that lies between the diamond anvils was preindented to 20 GPa and its thinnest part was removed. Then, a cubic BN/epoxy mixture powder was added inside the indent, which was then pressed to 20 GPa again, reliably insulating the sample and electrodes against the T301 gasket and serving as a quasihydrostatic pressure medium for the sample. Four electrodes were made of platinum foil with a thickness of 4 μm . The samples were cut into $380 \times 100 \times 25$ μm^3 chips, placed on top of the anvil, and pressed into the BN/epoxy layer together with the electrodes. The variation in pressure across the sample was less than 1 GPa in the studied pressure range. A ruby scale was used to determine the pressure through the optical window of the cryostat during the entire cooling process. In our experiments, pressure was generated by a pair of diamonds with 400 μm diameter tips. The electrodes and the gaskets were observed with a microscope in reflection light, and no contact between them was found at any stage in the experiments.

Crystallization often occurs via nucleation and growth processes when heating MGs and can greatly modify their properties. Thus, the crystallization behaviors of MGs are important in both their synthesis²⁸ and their applications.²⁹ Utilizing the HPHT-EDXRD technique, we studied the crystallization behaviors of the $\text{Ce}_{75}\text{Al}_{25}$ MG from about 0.1 to 4.2 GPa, which covers the pressure range in which the LDA to HDA $\text{Ce}_{75}\text{Al}_{25}$ MG polyamorphic transition occurs. Figures 1(a) and 1(b) show HPHT-EDXRD patterns of $\text{Ce}_{75}\text{Al}_{25}$ MG at 1.1 GPa and 3.0 GPa, respectively. Before crystallization, broad amorphous peaks are located at about 29.4 keV

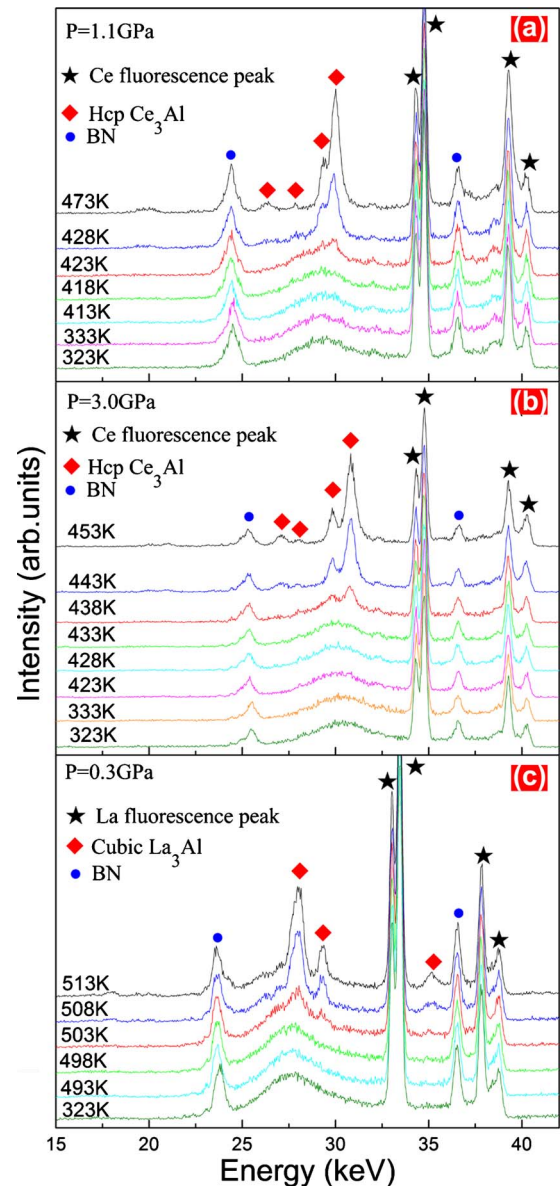


FIG. 1. (Color online) *In situ* HPHT-EDXRD patterns from $\text{Ce}_{75}\text{Al}_{25}$ MG, recorded at various temperatures under (a) 1.1 GPa and (b) 3.0 GPa and from $\text{La}_{75}\text{Al}_{25}$ MG under (c) 0.3 GPa. The crystallization phases for each sample are identical over the entire pressure range studied, and their diffraction peaks are marked by hcp Ce_3Al in (a) and (b) and cubic La_3Al in (c). Some other diffraction peaks for boron nitride, originating from the sample holder, are marked by BN, and four fluorescence peaks from Ce or La also are marked.

and about 30.3 keV under 1.1 GPa and 3.0 GPa, respectively, together with two Bragg peaks from the hexagonal BN and four fluorescence peaks from Ce. Two sharp Bragg peaks emerged over the broad amorphous peak, indicating the onset of crystallization at 423 K in Fig. 1(a) and at 438 K in Fig. 1(b), these temperatures are the estimated values of T_x . The $\text{Ce}_{75}\text{Al}_{25}$ MG crystallized into the same hcp Ce_3Al phase (space group $P6_3/mmc$), which is the stable phase for Ce_3Al at ambient pressure, in the entire studied pressure range of 0.1–4.2 GPa.³⁰ To clarify the effect of the $4f$ electrons,

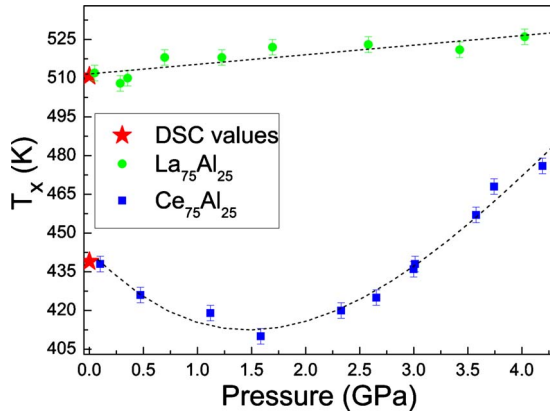


FIG. 2. (Color online) Crystallization onset temperatures T_x of $\text{Ce}_{75}\text{Al}_{25}$ and $\text{La}_{75}\text{Al}_{25}$ MGs as functions of pressure. The data at ambient pressure were estimated from the DSC measurements and are marked by red solid stars.

HPHT-EDXRD measurements were also performed on the $\text{La}_{75}\text{Al}_{25}$ MG. Figure 1(c) illustrates HPHT-EDXRD patterns of the $\text{La}_{75}\text{Al}_{25}$ MG at 0.3 GPa. The $\text{La}_{75}\text{Al}_{25}$ MG crystallized into its stable cubic La_3Al phase (space group $Pm\bar{3}m$) over the entire pressure range of 0.1–4.2 GPa. Figure 2 shows T_x as a function of pressure for the $\text{Ce}_{75}\text{Al}_{25}$ and $\text{La}_{75}\text{Al}_{25}$ MG. The applied pressure affects the T_x of both samples and the two samples exhibit different behaviors. The T_x of the $\text{Ce}_{75}\text{Al}_{25}$ MG initially decreases with increasing pressure, until 1.5 GPa, and then increases with increasing pressure, up to 4.2 GPa. This turning point at 1.5 GPa coincides with the reported LDA-to-HDA polyamorphic transition pressure of $\text{Ce}_{75}\text{Al}_{25}$ MG,¹⁸ which indicates the different thermodynamic properties (different crystallization mechanism) of the LDA and HDA $\text{Ce}_{75}\text{Al}_{25}$ MG. In contrast, the T_x of the $\text{La}_{75}\text{Al}_{25}$ MG exhibits a monotonic linear increase with increasing pressure, with a positive slope of about 3.7 K/GPa from 0.1 to 4.1 GPa. This result suggests that no LDA-to-HDA polyamorphic transition occurred in the $\text{La}_{75}\text{Al}_{25}$ MG, which is consistent with the smoothly decreasing volume of $\text{La}_{75}\text{Al}_{25}$ MG under high pressure.²²

The crystallization of MGs under high pressure is generally controlled by competition between the thermodynamic potential barrier of nucleation ΔG^* and the atomic diffusion activation energy Q_n , which includes the effects of pressure on the molar volume change, molar free energy change, the elastic energy induced by volume change, interfacial energy between the amorphous phase and its crystalline counterpart, and atomic mobility.³¹ In general, pressure could decrease T_x by reducing ΔG^* between the MG and its crystalline counterpart and increase T_x by depressing the atomic mobility (increasing Q_n).³¹ The negative dT_x/dP observed below 1.5 GPa in the $\text{Ce}_{75}\text{Al}_{25}$ MG sample could be controlled by a decreasing ΔG^* in the LDA $\text{Ce}_{75}\text{Al}_{25}$ MG phase, which is in contrast to the positive slope of the $\text{La}_{75}\text{Al}_{25}$ MG sample over this pressure range. However, above about 1.5 GPa, the T_x of both the $\text{Ce}_{75}\text{Al}_{25}$ and the $\text{La}_{75}\text{Al}_{25}$ MG samples increase with pressure. T_x has a slope of about 33 K/GPa in the $\text{Ce}_{75}\text{Al}_{25}$ MG (1.5–4.2 GPa), higher than the typical 0–30 K/GPa in other MGs in the pressure range of 0–4 GPa.^{23,31,32}

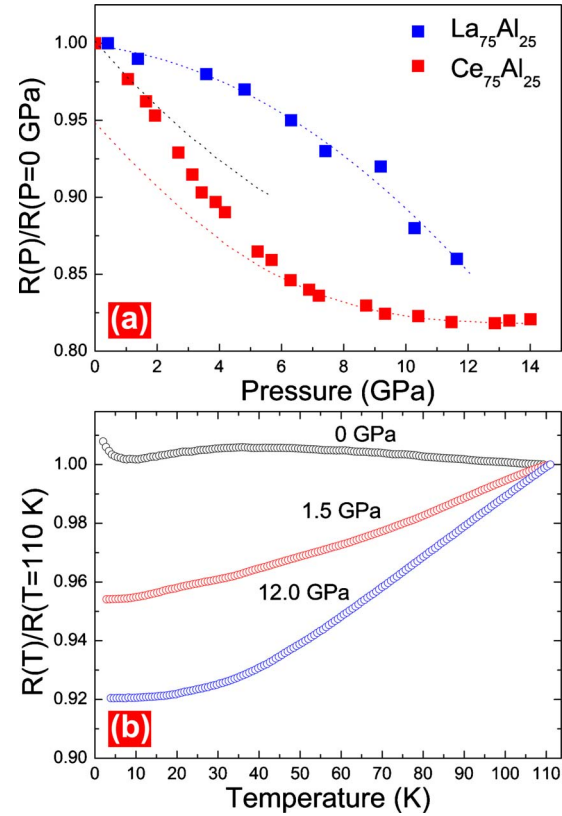


FIG. 3. (Color online) (a) Resistances of $\text{Ce}_{75}\text{Al}_{25}$ and $\text{La}_{75}\text{Al}_{25}$ MGs as functions of pressure at ambient temperature. (b) The temperature dependences of the resistance of $\text{Ce}_{75}\text{Al}_{25}$ MG at ambient pressure, 1.5 and 12 GPa.

Because the onset of the LDA-to-HDA transition in $\text{Ce}_{75}\text{Al}_{25}$ MG at 1.5 GPa is accompanied by $4f$ electron delocalization, which makes the electronic structure of Ce become similar to that of La, thus, it is reasonable that dT_x/dP is positive above 1.5 GPa for HDA $\text{Ce}_{75}\text{Al}_{25}$ MG. Furthermore, $4f$ electron delocalization causes a volume collapse (densification) in HDA $\text{Ce}_{75}\text{Al}_{25}$ MG (1.5–4.2 GPa). This densification effect of pressure is seldom in the MG systems studied before, which could cause a decrease in atomic mobility, i.e., an enhancement of activation energy Q_n , and consequently result in a large dT_x/dP of 33 K/GPa observed in the HDA $\text{Ce}_{75}\text{Al}_{25}$ MG.

Electronic transport properties were investigated through the relative resistance of the LDA and HDA $\text{Ce}_{75}\text{Al}_{25}$ MGs, shown in Fig. 3 together with $\text{La}_{75}\text{Al}_{25}$ MG for comparison. The resistance of the $\text{Ce}_{75}\text{Al}_{25}$ MG at ambient temperature, shown in Fig. 3(a), decreases with increasing pressure and exhibits a transition starting at about 2 GPa and ending at about 6 GPa, connected to two distinct states, which resemble the LDA-HDA transition observed through XRD.¹⁸ The relatively wide transition range should be caused by the quasihydrostatic pressure conditions of this experiment. [Note that helium as a best hydrostatic pressure medium was used in the XRD experiments.¹⁸ The gaps in data points in Fig. 3(a) were just caused by the accidental jumps of pressure (less than 1 GPa) during the pressure increasing via DAC screw rotation by hand.] For comparison, it was found

that the resistance of the $\text{La}_{75}\text{Al}_{25}$ MG does not exhibit an obvious transition as the $\text{Ce}_{75}\text{Al}_{25}$ MG does, although the resistance of the $\text{La}_{75}\text{Al}_{25}$ MG decreases with pressure. For their different curvatures of resistance vs pressure curves, we still do not know the exact origin, which might be caused by their different electronic structures (with and without $4f$ electron). According to Ziman-Faber theory, the resistance of a MG is primarily dominated by scattering from the intrinsically disordered atomic arrangements rather than thermal phonon scattering, which closely relates the resistivity to the scattering structure factor $S(q)$.^{33,34} Electrical properties are supposed to be sensitive (more so than XRD) to such an electronic-structure-based polyamorphic transition. However, the quasihydrostatic pressure conditions in this resistance experiment may mess it. Additionally, the pressure effect on resistance is very complex in MG, and generally depends on many factors, e.g., the pressure dependence of Fermi wave vector k_F , Fermi energy E_F , volume V , and structure factor at $q=2k_F$, $S(2k_F)$ and single-ion pseudopotential of the constituent atoms. Approximately, it is related to the linear compressibility.^{35–37} The resistance of the $\text{Ce}_{75}\text{Al}_{25}$ MG at 14 GPa decreased by about 18% from its value at ambient pressure, which is roughly consistent with the linear compressibility at 14 GPa (11%) estimated by XRD.¹⁸ To further reveal differences in the electronic transport properties of the LDA and HDA $\text{Ce}_{75}\text{Al}_{25}$ MGs, the temperature coefficient of resistance (TCR) of the $\text{Ce}_{75}\text{Al}_{25}$ MG was measured at three pressures and is shown in Fig. 3(b). The pressure in the DAC was found to be unstable during cooling until the temperature was below 110 K, as the DAC shrinks during cooling. Thus, only the data below 110 K are shown in Fig. 3(b). At ambient pressure, the LDA $\text{Ce}_{75}\text{Al}_{25}$ MG exhibits a negative TCR equal to about $-1 \times 10^{-4} \text{ K}^{-1}$, which is consistent with the typical TCR value in MGs.^{38,39} According to Ziman-Faber theory, this negative TCR indicates that $2k_F \approx k_p$ in LDA $\text{Ce}_{75}\text{Al}_{25}$ MG, where k_p is the position of the first peak in the static structure factor.^{33,38} The sample exhibits a resistance minimum at about 8 K, and then the resistance increases rapidly with decreasing T , which is attributed to the Kondo interaction between the local $4f$ electrons and the conduction electrons in Ce-bearing materials.³⁹ However, at 1.5 GPa the $4f$ electrons in the $\text{Ce}_{75}\text{Al}_{25}$ MG start to delocalize, resulting in a positive TCR of about $5 \times 10^{-4} \text{ K}^{-1}$ at 110 K. No Kondo effect feature is present; instead, a residual resistance plateau exists below 8 K. A similar disappearance of the Kondo feature at low temperature was reported in the crystalline intermetallic Ce_3Al compound under high pressure, which had been suggested to resemble the γ - α transition in Ce.⁴⁰ The HDA $\text{Ce}_{75}\text{Al}_{25}$ MG at 12 GPa, in which a

large fraction of $4f$ electrons delocalize, has a positive TCR of about $9 \times 10^{-4} \text{ K}^{-1}$, and the residual resistance plateau extends to about 20 K. The unique $4f$ electron delocalization during the LDA to HDA polyamorphic transition in $\text{Ce}_{75}\text{Al}_{25}$ at 1.5 GPa increases the number of conduction electrons, which may shift $2k_F$ away from k_p .³⁴ Consequently, the TCR can change from a negative value at ambient pressure to a positive value above 1.5 GPa. This kind of pressure-tuned TCR from a negative to a positive value in MGs under pressure is seldom observed before. These property changes are also reversible, as is the electronic polyamorphic transition in Ce-bearing MGs.^{16,20}

In conclusion, using *in situ* HPHT-EDXRD and *in situ* high-pressure, low-temperature, four-probe resistance measurements, we have observed changes in the thermodynamic and electronic transport properties accompanying the polyamorphic transition in the $\text{Ce}_{75}\text{Al}_{25}$ MG. This transition is linked to the unique $4f$ electron delocalization in Ce-bearing MGs. Below 1.5 GPa, for the LDA $\text{Ce}_{75}\text{Al}_{25}$ MG, dT_x/dP is negative and becomes positive above 1.5 GPa after the transition to the HDA $\text{Ce}_{75}\text{Al}_{25}$ MG, although the same crystalline phase was detected over the entire pressure range studied. In resistance measurements at ambient temperature, the HDA $\text{Ce}_{75}\text{Al}_{25}$ MG exhibits a lower resistance than the LDA $\text{Ce}_{75}\text{Al}_{25}$ MG. A pressure-tuned TCR, which shifted from negative to positive values, was observed during the polyamorphic transition in $\text{Ce}_{75}\text{Al}_{25}$ MG. These results have revealed that the LDA and HDA $\text{Ce}_{75}\text{Al}_{25}$ MG phases do have different properties, which will trigger further investigations into fabricating HDA MGs with interesting properties.

We thank C. L. Qin (Institute for Materials Research, Tohoku University, Sendai, Japan) for the starting material synthesis. This research was supported by National Natural Science Foundation of China under Grants No. 50701038, No. 60776014, No. 60876002, No. 10874053, No. 50871104, No. 50920105101, No. 10979002, and No. 51050110136, Zhejiang Provincial Natural Science Foundation (Grant No. Y4080324), the Balzan Foundation, U.S. Department of Energy (DOE), Office of Science, Office of Basic Energy Sciences (BES) under Award No. DE-FG02-02ER45955, the National Basic Research foundation of China (Grant No. 2005CB724404), the Zhejiang University-Helmholtz Cooperation Fund, the Ministry of Education of China (Changjiang foundation), the Department of Science and Technology of Zhejiang Province, and the Baoyugang foundation of Zhejiang University. This research is also supported as part of EFree, an Energy Frontier Research Center funded by DOE-BES under Award No. DE-SC0001057.

*qiaoshizeng@gmail.com

†jiangjz@zju.edu.cn

¹A. L. Greer and E. Ma, *MRS Bull.* **32**, 611 (2007).

²A. Inoue and N. Nishiyama, *MRS Bull.* **32**, 651 (2007).

³P. H. Poole, T. Grande, C. A. Angell, and P. F. McMillan, *Science* **275**, 322 (1997).

⁴P. F. McMillan, *J. Mater. Chem.* **14**, 1506 (2004).

⁵C. A. Tulk, R. Hart, D. D. Klug, C. J. Benmore, and J. Neufeind, *Phys. Rev. Lett.* **97**, 115503 (2006).

⁶O. Mishima and Y. Suzuki, *Nature (London)* **419**, 599 (2002).

⁷J. P. Itie, A. Polian, G. Calas, J. Petiau, A. Fontaine, and H. Tolentino, *Phys. Rev. Lett.* **63**, 398 (1989).

- ⁸S. K. Lee, P. J. Eng, H. K. Mao, Y. Meng, and J. Shu, *Phys. Rev. Lett.* **98**, 105502 (2007).
- ⁹C. Meade, R. J. Hemley, and H. K. Mao, *Phys. Rev. Lett.* **69**, 1387 (1992).
- ¹⁰E. Soignard, S. A. Amin, Q. Mei, C. J. Benmore, and J. L. Yarger, *Phys. Rev. B* **77**, 144113 (2008).
- ¹¹M. Guthrie, C. A. Tulk, C. J. Benmore, J. Xu, J. L. Yarger, D. D. Klug, J. S. Tse, H.-k. Mao, and R. J. Hemley, *Phys. Rev. Lett.* **93**, 115502 (2004).
- ¹²W. A. Crichton, M. Mezouar, T. Grande, S. Stolen, and A. Grzechnik, *Nature (London)* **414**, 622 (2001).
- ¹³Q. Mei, C. J. Benmore, R. T. Hart, E. Bychkov, P. S. Salmon, C. D. Martin, F. M. Michel, S. M. Antao, P. J. Chupas, P. L. Lee, S. D. Shastri, J. B. Parise, K. Leinenweber, S. Amin, and J. L. Yarger, *Phys. Rev. B* **74**, 014203 (2006).
- ¹⁴P. F. McMillan, M. Wilson, D. Daisenberger, and D. Machon, *Nature Mater.* **4**, 680 (2005).
- ¹⁵H. W. Sheng, W. K. Luo, F. M. Alamgir, J. M. Bai, and E. Ma, *Nature (London)* **439**, 419 (2006).
- ¹⁶H. W. Sheng, H. Z. Liu, Y. Q. Cheng, J. Wen, P. L. Lee, W. K. Luo, S. D. Shastri, and E. Ma, *Nature Mater.* **6**, 192 (2007).
- ¹⁷Q. S. Zeng, Y. C. Li, C. M. Feng, P. Liermann, M. Somayazulu, G. Y. Shen, H. K. Mao, R. Yang, J. Liu, T. D. Hu, and J. Z. Jiang, *Proc. Natl. Acad. Sci. U.S.A.* **104**, 13565 (2007).
- ¹⁸Q. S. Zeng, Y. Ding, W. L. Mao, W. G. Yang, S. V. Sinogeikin, J. F. Shu, H. K. Mao, and J. Z. Jiang, *Phys. Rev. Lett.* **104**, 105702 (2010).
- ¹⁹X. R. Liu and S. M. Hong, *Appl. Phys. Lett.* **90**, 251903 (2007).
- ²⁰Q. S. Zeng, Y. Ding, W. L. Mao, W. Luo, A. Blomqvist, R. Ahuja, W. Yang, J. Shu, S. V. Sinogeikin, Y. Meng, D. L. Brewster, J. Z. Jiang, and H. K. Mao, *Proc. Natl. Acad. Sci. U.S.A.* **106**, 2515 (2009).
- ²¹Y. Z. Guo and M. Li, *Appl. Phys. Lett.* **94**, 051901 (2009).
- ²²H. W. Sheng, E. Ma, H. Z. Liu, and J. Wen, *Appl. Phys. Lett.* **88**, 171906 (2006).
- ²³J. Z. Jiang, T. J. Zhou, H. Rasmussen, U. Kuhn, J. Eckert, and C. Lathe, *Appl. Phys. Lett.* **77**, 3553 (2000).
- ²⁴D. L. Decker, *J. Appl. Phys.* **42**, 3239 (1971).
- ²⁵M. I. Eremets, V. W. Struzhkin, H. K. Mao, and R. J. Hemley, *Science* **293**, 272 (2001).
- ²⁶K. Shimizu, K. Suhara, M. Ikumo, M. I. Eremets, and K. Amaya, *Nature (London)* **393**, 767 (1998).
- ²⁷Y. H. Han, C. X. Gao, Y. Z. Ma, H. W. Liu, Y. W. Pan, J. F. Luo, M. Li, C. Y. He, X. W. Huang, and G. T. Zou, *Appl. Phys. Lett.* **86**, 064104 (2005).
- ²⁸M. G. Scott, in *Amorphous Metallic Alloys*, edited by F. E. Luborsky (Butterworths, Boston, 1983), p. 144.
- ²⁹K. Lu, *Mater. Sci. Eng. R.* **16**, 161 (1996).
- ³⁰A. C. Lawson, J. M. Lawrence, J. D. Thompson, and A. Williams, *Physica B* **163**, 587 (1990).
- ³¹Y. X. Zhuang, J. Z. Jiang, T. J. Zhou, H. Rasmussen, L. Gerward, M. Mezouar, W. Crichton, and A. Inoue, *Appl. Phys. Lett.* **77**, 4133 (2000).
- ³²J. Z. Jiang, J. S. Olsen, L. Gerward, S. Abdali, J. Eckert, N. Schlorke-de Boer, L. Schultz, J. Truelsen, and P. X. Shi, *J. Appl. Phys.* **87**, 2664 (2000).
- ³³J. M. Ziman, *Philos. Mag.* **6**, 1013 (1961).
- ³⁴L. V. Meisel and P. J. Cote, *Phys. Rev. B* **15**, 2970 (1977).
- ³⁵G. Fritsch, W. Dyckhoff, W. Pollich, and E. Luscher, *J. Phys. F: Met. Phys.* **15**, 1537 (1985).
- ³⁶G. Fritsch, J. Willer, A. Wildermuth, and E. Luscher, *J. Phys. F: Met. Phys.* **12**, 2965 (1982).
- ³⁷D. Lazarus, *Solid State Commun.* **32**, 175 (1979).
- ³⁸P. J. Cote and L. V. Meisel, *Phys. Rev. Lett.* **39**, 102 (1977).
- ³⁹M. B. Tang, H. Y. Bai, W. H. Wang, D. Bogdanov, K. Winzer, K. Samwer, and T. Egami, *Phys. Rev. B* **75**, 172201 (2007).
- ⁴⁰Y. Y. Chen, J. M. Lawrence, J. D. Thompson, and J. O. Willis, *Phys. Rev. B* **40**, 10766 (1989).